Path Calibration and Regional Discriminants in North Africa and the Middle East

Chandan K. Saikia (PI) and B. B. Woods (Co-PI)
Woodward-Clyde Federal Services
Pasadena, CA 91101

Contract F19628-95-C-0093
Sponsored by ARPA

ABSTRACT

Reviews on the effectiveness of regional discriminants suggest that discriminant rules developed for one region do not readily apply to another. However, it is feasible to apply these discriminants in a new region provided relative path corrections for various seismic phases (i.e., P_n, L_g, and R_g) are available. We are presently investigating path corrections for the North Africa and other Middle East regions around the GSETT-3 stations. Our objective is to develop regional magnitude relationships using the amplitude distance corrections that will be obtained from the crustal models. To this end, regional broadband seismograms recorded by the operational GSETT-3 stations in these regions will be modeled by calibrating the regional waveguide to establish path corrections for individual phases. For those GSETT-3 stations which have not become operational yet, regional seismograms from the nearby WWSSN stations will be analyzed. Whenever possible, we will select large earthquakes which are recorded regionally and teleseismically, and for which their focal mechanisms have been determined previously. To date, we have collected regional waveforms recorded at KEG (Kottamiya, Egypt, operating since 1990), HLW (Halwan, Egypt) and KIV (Kislovodsk, CIS), and modeling of these waveforms has just started. This study also includes finding path corrections for regional phases around a newest GSETT-3 array, PAKO deployed near Nilore (NIL, location of a former WWSSN station) in Pakistan. This array is also located southwest of a recent PASCAL experiment which consisted of nine broadband stations. Initial success in modeling regional seismograms from this PASCAL experiment is quite promising and we have already obtained a preliminary crustal structure model near the PAKO array. Based on this initial crustal structure, we present results discussing various trade-offs between depth and focal mechanism for observed earthquakes and demonstrate that these trade-offs are real by comparing our preferred solutions with those of CMT.

OBJECTIVES

A recent review of effective regional discriminants and their transportability indicates that a discriminant rule established in one region does not readily apply to another (Fisk et al., 1994); consequently, establishing relative path corrections for the various phases (P_n, L_g, R_g etc.) are essential for new regions. To this end, we are calibrating paths in North Africa and other Middle East regions for the IDC event indentification subsystem. We envision providing travel-time and amplitude-distance curves or relations for each of the GSETT-3 stations operating in these regions. Directly related to the amplitude distance corrections are regional magnitude relationships which will also be developed. We will determine short-period magnitude relationships for P_n ($m_b(P_n)$), $L_g(m_b(L_g))$, and $S_g(m_b(S_g))$ vs distance. We will also estimate the effective t* beneath our source region by comparing teleseismic and regional derived source histories. Special calibrations to ARPA's short-period arrays with respect to regional source strengths will be established. Such t* values will then be used to predict teleseismic m_b and obtain a calibration for regional m_b versus teleseismic m_b.

Developing the above travel-time and amplitude-magnitude distance curves involves waveform modeling of regional seismograms and advanced processing techniques for regional array data, such as modeling of specific depth phases, as well as developing softwares for automated real-time source discrimination routines. While small earthquakes ($m_b < 4.5$) can cause difficulties in discrimination, larger events ($m_b > 5.5$) can be used to calibrate paths and establish source estimation techniques useful for all sizes of events. Our strategy is to find a set of intermediate to large magnitude earthquakes in the study regions which have been recorded both regionally and teleseismically with the emphasis placed on events recorded by GSETT-3 stations or by stations located near the proposed GSETT-3 sites. Accurate source parameters can be obtained from the teleseismic observations and these earthquakes can be used as "teleseismic master" events. The composition of teleseismic down-going P and up-going pP waves can be modeled for each teleseismic master event to determine source complexity and depth. Using these derived source parameters, broadband characteristics of P_{nl}, S_{nl} and surface waves recorded on regional waveforms consequently can be modeled for calibration of source to receiver paths. After calibrating these regional paths, regional waveforms recorded from other smaller events are inverted to determine their source mechanism and seismic moment M_o. For the purpose of path calibration around the GSETT-3 stations, we are also looking for a set of "regional master" earthquakes when the teleseismic ones are not available. These earthquakes must be recorded with good signal to noise ratio. We use long-period regional seismograms from the "regional masters" and a simplified initial crustal structure consistent with the local geology to determine source parameters. Once source mechanisms are determined, the regional long-period data can be modeled to improve the crustal structure. Structure models obtained

from the long-period records are later refined to fit the short-period signals which are observed in the broadband data. We shall also invert for the broadband source time function for each of these regional events. We expect regional master events to be small but of large enough magnitude to be recorded by various operational arrays at teleseismic distances. We shall stack P waveforms recorded by these arrays to enhance the signal quality and will attempt to model the enhanced P wave by convolving the inverted source time function with a suitable t* operator.

An additional focus of this study is to further develop energy-based regional discriminants that can be integrated into an operational environment to monitor North Africa and the Middle East (including western Iran, the southern-most states of the former Soviet Union and Pakistan). The main difficulty in applying discriminants to these regions is the recognition of a "first blast", since these regions have high natural seismicity but few, if any, large explosions. Besides calibrating these regions with respect to regional and teleseismic phases, we intend to test the applicability of regional discriminants we developed using earthquakes and explosions from western United States and many parts of central Asia (Woods et al., 1993; Woods and Saikia, 1995) and investigate the factors influencing their transportability. It should be noted that parameters obtained from modeling regional seismograms are used to determine the following regional discriminants: M_L vs M_o and M_E/M_B:M_o or M_E:M_B vs M_o where M_E is the energy required to match the total energy in the recorded data to that in the synthetic waveforms and M_B is the moment determined by modeling broadband P_{nl} data.

PRELIMINARY RESULTS

One of the newest arrays to be developed is in Pakistan, PAKO. It is located just southwest of a recent PASCAL experiment near the old WWSSN station NIL (Nilore) as displayed in Figure 1. Thus this broadband array provides an excellent opportunity to examine the wave propagation characteristics of this region. The array was operated only for a few months, September to December 1992, but recorded a number of significant events since this region is seismically very active (Ni et al., 1993). Some preliminary mechanisms are displayed in Figure 1 indicating strike-slip type mechanism expected from the west and mixed mechanisms from the north. These latter events are from the Hindu-Kush region and generally show such diversity in depth and mechanisms (Chatelain et al., 1980). This event diversity was also found in a recent study of the broadband regional recordings from GAR, see Figure 1. Zhao and Helmberger (1993) derived two crustal models for the region, one with uniform crust and one containing a gradient. A similar but simpler model is displayed in Table 1 which proved effective in modeling events beneath Tibet, Zhu and Helmberger (1995) of this report.

As discussed in Song and Helmberger (1995) one can generally model regional records at frequencies above a few Hz for ranges from 300 to 800 km with very simple two layer models. The top layer controls the surface waves while the moho controls the body phases. Since we are beyond critical angle, the relative sharpness of the crust mantle transition is not important. Crustal gradients do affect the time separation between the P_{nl} waves (extended P wave), the S_{nl} and surface waves, but this effect can be handled by the so-called "cut-and-paste" method of Zhao and Helmberger (1994). This method uses a direct grid-search approach and matches the complete seismograms against synthetic over discrete phases, so that timing shift between particular arrivals are allowed. This feature eliminates the need for an accurate crustal model for computing the fundamental Green's functions. Figure 2 and 3 display the fits obtained by this method. To improve the method, we introduce more sensitivity to amplitudes by fitting absolute motions, see Zhu and Helmberger (1995) of this report. Thus, examining the SH waves one can easily see the enhancement of amplitudes going from stations SHAB to DASU where the latter is near the maximum of the radiation pattern. Note that the Pnl's have been fit separately as discussed above. The model appears to be too slow for this region and so the complete synthetics have been shifted 4s forward in Figure 2 and 3s in Figure 3. The additional shifts are then made per trace. For the Pnl synthetics at SHAB has been shifted a total of 5.8s, or the synthetic is late by 5.8s. Note that the path to DASU is only 4.4s late. The observed love wave is 8.8s early relative to the synthetics, etc. At this stage these shifts are viewed as a base-line since we do not necessarily know the origin time. Trade-offs between depth and origin time is discussed in Zhao and Helmberger (1991). They find that throughout the Tibetan Plateau region events systematically are located too deep by about 20 km and occur about 4s earlier than given in PDE estimates.

These events are too small to be well recorded teleseismically and do not have CMT type solutions. One of the crustal events studied to date does have a Harvard solution, namely the 328.2 (M=5.6) event. Their mechanism versus our estimates are given in Figure 4 where we have tested four depths, 10, 20, 30 and 40 kms. The best fits occur for depths 10 and 20 kms, while the fits for depths 30 and 40 kms yield about double the error. These results are essentially a simple station solution given the azimuth of the event and these trade-offs of mechanism versus depths appear to be real as discussed in Zhao and Helmberger (1993). The CMT depth determination was 43 km, but this must be checked since their solutions have a 20 km bias in this region as determined from identifying depth phases in teleseismic body waves, see Zhao and Helmberger (1993). Deep events are particularly simple at these ranges and occur often in this region. An example is displayed in Figure 5. This event is near M=5 and causes some difficulty in m_b:M_s discrimination because the surface waves are relatively small. Teleseismically, an event of this size can also be difficult to analyze since depth phases become less obvious, see Figure 6. Short-period array stacks could prove very helpful for such events

and this type of data will be added to our source inversion technique in the near future.

REFERENCES

Fisk, M. D., G. L. Henry and G. D. McCartor (1994). Preliminary assessment of seismic CTBT/NPT monitoring capability, Scientific Report No 1. PL-TR-94-2300, 39p. ADA293188

Ni, J. F., A. Ibenbrahim and S. W. Roecker (1991). Three-dimensional velocity structure and hypocenters of earthquakes beneath the Hazara Arc, Pakistan: Geometry of the underthrusting Indian Plate, J. Geophys. Res., Vol 94, 19,865-19,877.

Song, X. and D. V. Helmberger (1995). Broadband modeling of regional seismograms: the basin and range crustal structure, submitted to Bull. Seis. Soc. Am.

Woods, B. B., S. Kedar, and D. V. Helmberger (1993). ML:Mo as regional seismic discriminant, Bull. Seis. Soc. Am., 83, pp 1167-1183.

Woods, B.B. and C. K. Saikia (1995). The portability of some regional seismic discriminants and related broadband waveform monitoring, Paper presented in the 17th Annual Research Symposium on CTBT monitoring at Scottsdale, Arizona. PL-TR-95-2108

Zhao, L. Z. and D. V. Helmberger (1991). Geophysical implication from relocations of Tibetan earthquakes - Hot lithosphere, Geophys. Res. Lett. 18, pp 2205-2208.

Zhao, L. Z. and D. V. Helmberger (1993). Source retrieval from broadband regional seismograms: Hindu-Kush region, Phys. Earth Planet. Inter., 78, 69-95, 1993.

Zhao, L. Z. and D. V. Helmberger (1994). Source estimation from broadband regional seismograms, Bull Seis. Soc. Am., 84, 91-104.

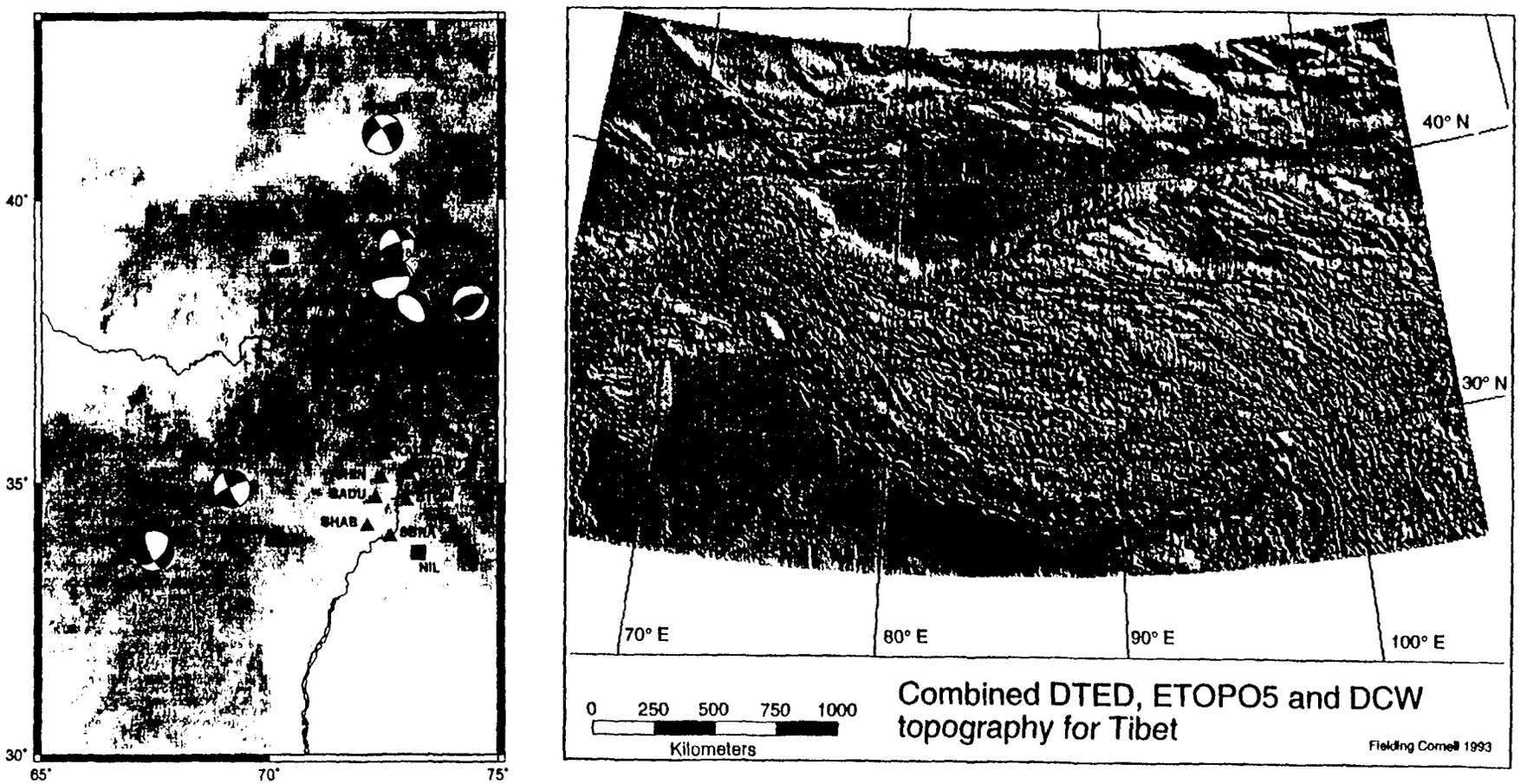

Figure 1. Panel on the right displays the shaded relief for the Tibet region, after Fielding et al. (1993) and panel on the left displays the PASCAL array location relative to NIL (PAKO), the IRIS station GAR (now closed down) and a number of events.

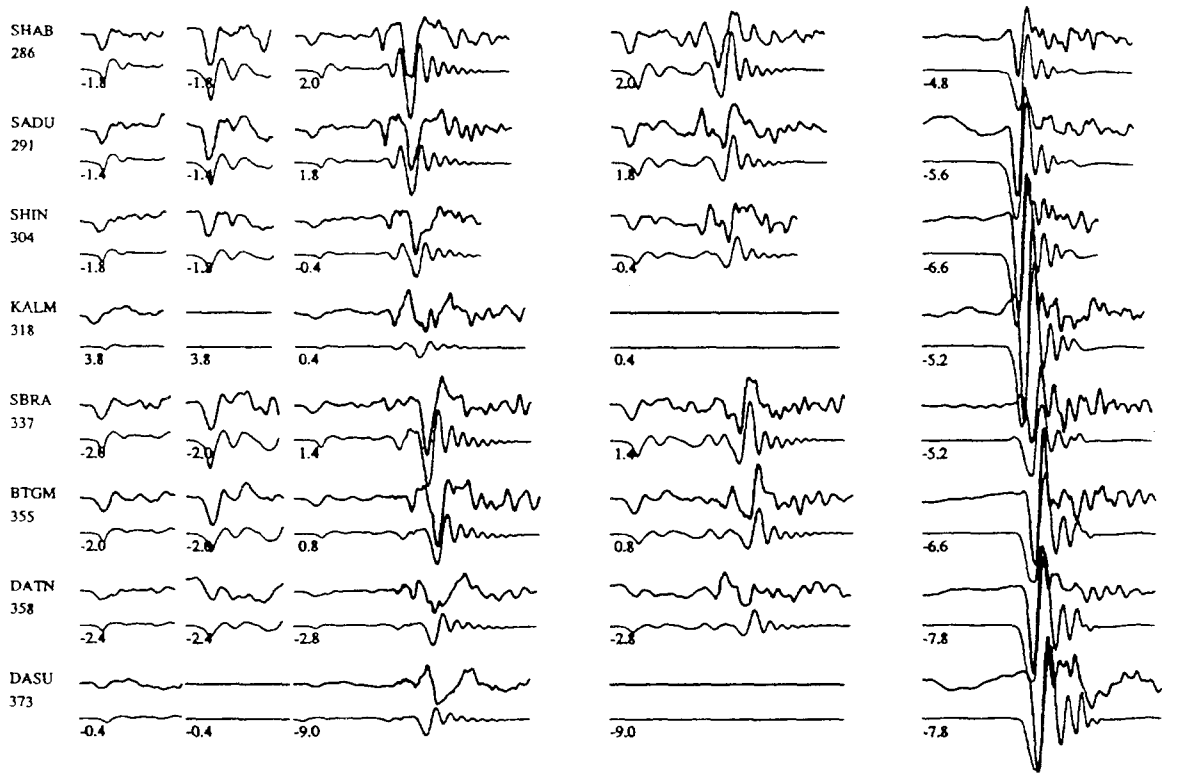

Figure 2. Comparison of synthetics and observations for the 311.1758 event (M=5). The synthetics and observations are relative to SHAB (Peak-to-peak amplitude of tangential is 0.011 Qcm). The seismic moment estimate is 7.9×10^{23} ergs, depth of 10 km, strike, dip and rake (70°, 90°, 230°).

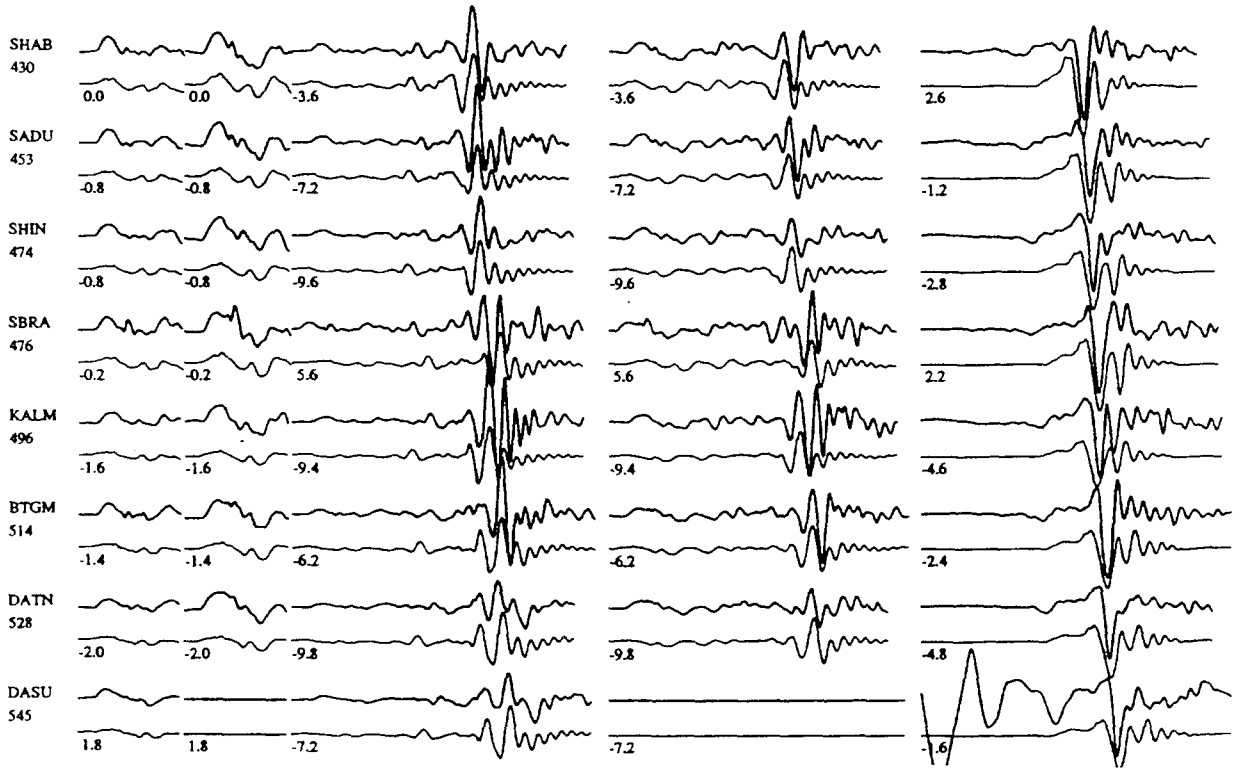

Figure 3. Comparison of synthetics and observations for 322.0238 event, $M_o=3.2 \times 10^{24}$ ergs, h=10 kms, mechanism (30°, 50°, 250°), peak-to-peak amplitude at SHAB tangential is 0.0042 cm.

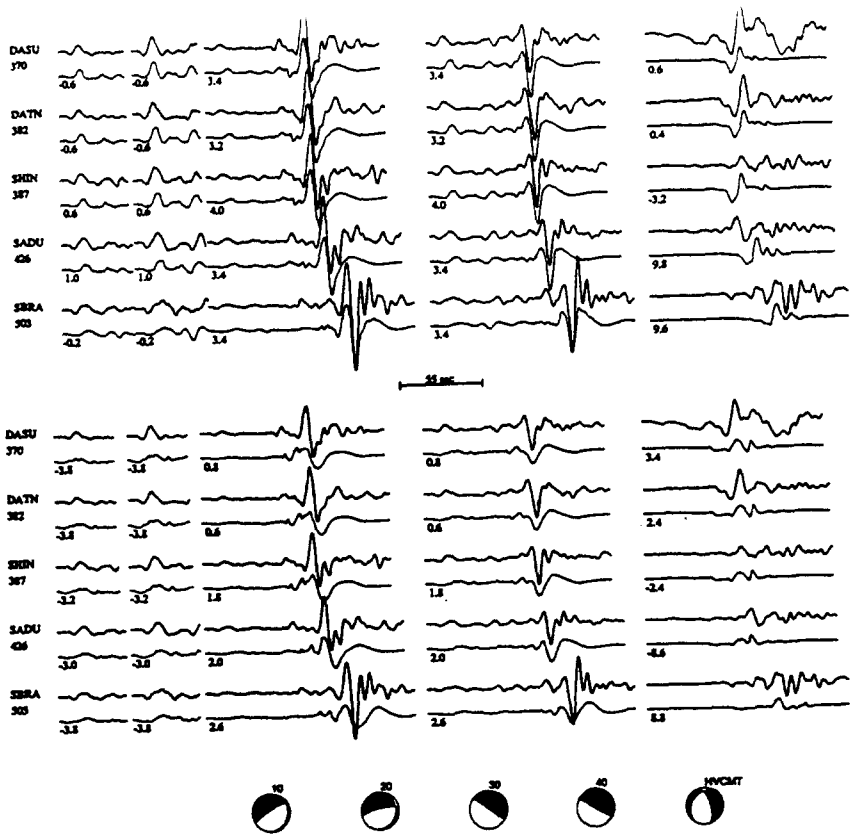

Figure 4. Comparison of solutions of the 328.2311 event (M=5.6) with the CMT solution. Upper panel displays results assuming a depth of 20 km (M_o=6.3 x 10^{24} ergs). Lower panel displays results for a depth of 40 km (M_o= 8.9 x 10^{24} ergs).

Figure 5. Comparison of observations and synthetics for a deep event (h=150 kms), 276.1438.

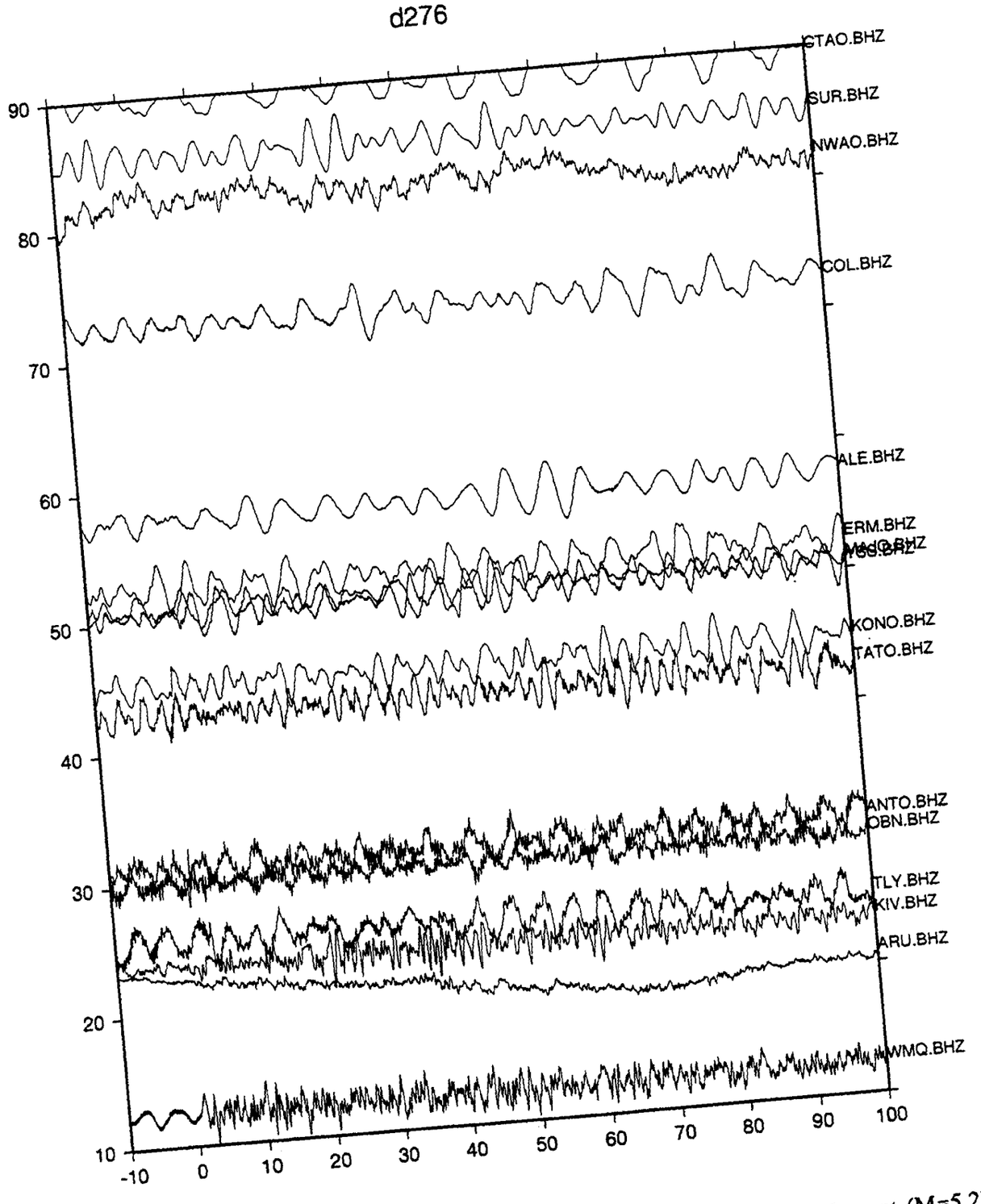

Figure 6. Output of FARM preview of IRIS data, vertical broadband for the 276 event (M=5.2) displayed in Figure 5. Only a few stations have useful data.

Table 1. Average velocity model of the Tibetan Plateau

layer	Thickness (km)	V_p (km/s)	V_s (km/s)
1	4	4.70	2.70
2	60	6.20	3.50
3	–	8.14	4.70

Table 2. Locations of the events from PDE catalog

Event	Date	Origin time	*lat.*	*lon.*	h (km)	M_b
355	12-21-91	$19^h52^m45.5$	27.90N	88.14E	57	4.9
067	03-07-92	$22^h41^m50.8$	29.44N	89.37E	113	4.3
095	04-04-92	$17^h43^m20.7$	28.15N	87.98E	33	4.9

Table 3. Focal depths and fault plane solutions from waveform modeling

Event	P axis [a]	T axis [a]	h (km)	M_w
355	341±9/57± 8	81±7/ 6± 4	75±10	4.9
067	225±4/31±10	125±4/16±11	75±10	4.4
095	8±7/30± 9	270±9/18± 9	75±10	4.9

[a] Azimuth/Plunge, all in degrees